

The Effect of Immersion Time and Immersion Temperature on the Corrosion Behavior of Zinc Phosphate Conversion Coatings on Carbon Steel

Vahid Asadi^a, Iman Danaee^{a*}, Hadi Eskandari^a

^aAbadan Faculty of Petroleum Engineering, Petroleum University of Technology, Abadan, Iran

Received: October 30, 2014; Revised: July 29, 2015

The formation and corrosion performance of zinc phosphate coating on carbon steel at different temperatures and immersion times was studied. The corrosion performance of coatings was investigated using potentiodynamic polarization and electrochemical impedance spectroscopy. The characterization and composition of coatings were studied by SEM and EDS analysis. The corrosion resistance in 3.5%wt. NaCl solution was increased in the presence of zinc phosphate conversion coatings. The effect of immersion time and coating temperature were studied on anti-corrosion behavior of coatings. Coating temperature showed a significant effect in phosphate conversion coating and higher corrosion resistance was obtained with 45 °C operating temperature. Also the experimental results indicated that the corrosion resistance increased with increasing the immersion time. This behavior can be related to the increase of the phosphate coating continuity which formed on the surface. Surface analysis results indicated that the coating obtained from 20 min immersion time was more uniform and continuous.

Keywords: zinc phosphate coating, corrosion, impedance, SEM

1. Introduction

Carbon steel, the most widely used engineering material, accounts for approximately 85% of the annual steel production worldwide. Despite its relatively limited corrosion resistance, carbon steel is used in large tonnages in marine applications, chemical processing, petroleum production and refining, construction and metal processing equipment^{1,2}. The economic consequences of corrosion of iron and its alloys in various industrial sectors, including oil and gas operations, are investigated³. There are different ways to control corrosion including inhibitors, coatings, applying anodic/cathodic protection and proper design⁴. Surface treatment is an effective technique to solve the problem, which includes chemical conversion coating,⁵⁻⁹ electroplating and electroless plating,^{10,11} physical vapor deposition^{12,13} and so on. Among these surface treatments, chemical conversion treatment is a simple and cost effective method and has been increasingly used in a wide range of applications.

Phosphating is the most widely used metal pre-treatment process for the surface treatment and finishing of ferrous and non-ferrous metals¹⁴⁻¹⁸. Phosphating has become popular because of its ability to improve adhesion of the organic topcoat and prevention of underfilm corrosion¹⁹. The main applications of phosphating are for increasing corrosion resistance, paint adhesion and promoting electrical insulation²⁰. The most commonly used phosphate coatings for corrosion protection are based on zinc, iron, and manganese²¹.

The phosphate coatings are formed by chemical reaction after immersing the metal in a solution containing soluble

primary metal phosphates, free phosphoric acid, various accelerators and modifiers²². In the zinc phosphating of carbon steel, when the metal surface is subjected to the bath, iron will be dissolved due to presence of phosphoric acid at microanodic sites. The hydrogen evolution has occurred on microcathodic sites and pH increase in the metal solution interface simultaneously. This leads to equilibrium between the soluble primary phosphates to insoluble tertiary phosphate on the surface.

In a zinc phosphating bath these equilibrium may be represented as:



A certain amount of free phosphoric acid must be present to repress the hydrolysis and to keep the bath stable for effective deposition of phosphate at the microcathodic sites^{23,24}. Temperature and immersion time are main effective parameters in zinc phosphate conversion coatings²³.

In this work, zinc phosphate conversion coating was deposited on carbon steel by chemical method in different temperatures and immersion times. The surface morphology of phosphate coating samples was assessed by scanning electron microscope (SEM) and the composition of the coating surface was evaluated by EDS analysis. Corrosion resistance of these coatings was investigated by polarization curve and electrochemical impedance spectroscopy (EIS) in 3.5% sodium chloride solution.

*e-mail: danaee@put.ac.ir

2. Experimental Details

2.1. Deposition process of zinc phosphating coating on carbon steel

Carbon steel substrates with composition in: C: 0.95; N: 3.02; O: 4.82; Al: 0.68; Si: 0.7; P: 0.15; S: 0.14; Mn: 0.73; St: 0.17; Cr: 0.01 wt. %; Fe: balance, were used for the deposition of phosphate coatings. The compositions of the phosphate baths used in this study were: H_3PO_4 (17 ml l⁻¹), ZnO (2 g l⁻¹) and NaOH with final pH=2.90 to 3.

After grinding and polishing, specimens were rinsed with deionized water then were immersed in the bath that maintained at special temperature for particular time, immediately. A gray coating with bright crystalline spots was formed on the substrate. After phosphating, the coated samples were rinsed with deionized water to remove residual acid and salts from the bath and dried with compressed air and then exposed to ambient temperature for some hours.

2.2. Evaluating of corrosion performance

The working electrode samples were mounted by a polymeric resin and the surface of 1cm² was obtained. The electrochemical studies were performed by polarization curves and electrochemical impedance spectroscopy, using Autolab PGSTAT 302N. A three electrode cell with Pt as counter and saturated Ag/AgCl as reference electrode was employed for this measurements. To reach the steady state condition, before each experiment, the working electrode was immersed in the test cell for 20 min. The measurements were repeated three times for each condition to ensure the reliability and reproducibility of the data. Polarization measurements were conducted in a 3.5% NaCl solution at room temperature with potential scan rate of 1 mV s⁻¹. Electrochemical impedance spectroscopies (EIS) were carried out at open circuit potential with AC amplitude of 10 mV over a frequency range of 100 kHz to 10 mHz. Fitting of experimental impedance spectroscopy data to the proposed equivalent circuit was done by means of a home written least square software based on the Marquardt method for the optimization of functions and Macdonald weighting for the real and imaginary parts of the impedance^{25,26}.

2.3. Surface characteristics of coating

By visual appearance, the color of the zinc phosphate coatings was grayish with bright crystalline spots. The surface morphology of zinc phosphate coated samples was assessed by scanning electron microscope model VGEA\TESCAN

equipped with energy dispersive X-ray and after polarization test by scanning electron microscope model JSM-840 (JEOL).

3. Results and Discussion

3.1. Effect of different temperature on corrosion performance

The polarization curves of steel electrode without and with phosphate coatings in 3.5% NaCl solution are given in Figure 1. Coatings were obtained by 20 min immersion time in the phosphating bath at different temperature. The electrochemical data including B_a , B_c , I_{corr} , E_{corr} , R_p and corrosion rate of each sample are reported in Table 1. It should be noted that the results were calculated by using Tafel extrapolation method. The Stern-Geary equation is used to calculate the R_p ²⁷:

$$I_{corr} = (1/2.303R_p) (B_a B_c / B_a + B_c) \quad (3)$$

Due to the insulating nature of phosphate coatings, these coatings provide an effective physical barrier to protect metals and significantly decrease the corrosion rate. In the NaCl solution, the predominant reactions that can occur during

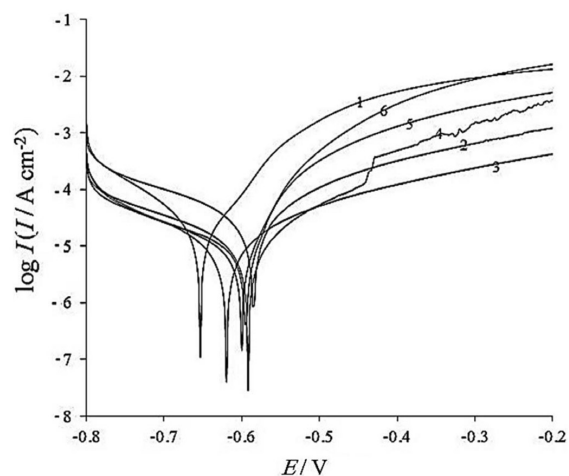


Figure 1. Polarization curves of steel electrode with and without zinc phosphate conversion coatings. Conversion coatings were obtained by 20 min immersion time in phosphate solution in different temperatures: 1) uncoated, 2) 20 °C, 3) 45 °C, 4) 55 °C, 5) 65 °C, 6) 80 °C.

Table 1. Potentiodynamic polarization parameters of different operating temperature for the phosphate coatings in 3.5 wt. % NaCl solution. Coatings were prepared by 20 min immersion time in phosphate solution.

Phosphate coating	B_a ($\pm 10^{-3}$) / V dec ⁻¹	B_c ($\pm 10^{-3}$) / V dec ⁻¹	I_{corr} ($\pm 5 \times 10^{-7}$) / A cm ⁻²	E_{corr} ($\pm 10^{-3}$) / V	R_p (± 5) / ohm	Corr.rate ($\pm 10^{-3}$) / mpy
uncoated	0.114	0.094	2.89×10^{-5}	-0.653	772.995	3.39×10^{-1}
20 °C, 20 min	0.2	0.15	2.78×10^{-5}	-0.585	1336.216	3.27×10^{-1}
45 °C, 20 min	0.137	0.110	6.49×10^{-6}	-0.620	4078.901	7.62×10^{-2}
55 °C, 20 min	0.205	0.136	1.04×10^{-5}	-0.592	3397.255	1.22×10^{-1}
65 °C, 20 min	0.188	0.066	8.68×10^{-6}	-0.600	2443.455	1.02×10^{-1}
80 °C, 20 min	0.195	0.042	7.59×10^{-6}	-0.595	2157.797	8.92×10^{-2}

the cathodic and anodic polarization are the reduction of oxygen and iron dissolution, respectively¹⁴.

As shown in Figure 1, phosphate coated samples have more positive corrosion potential, lower corrosion current density and higher polarization resistance. This indicates that the corrosion resistance of carbon steel improves by the phosphating treatment. Moreover, the anodic and cathodic processes of carbon steel corrosion suppress effectively by the complete coverage of phosphate coatings. As shown in Table 1, the phosphate coatings prepared at 45 °C shows the highest polarization resistance and the lowest corrosion current density due to the compact structure of coating. It was reported that slow reaction during zinc phosphating causes the more formation of phosphophyllite (iron-zinc phosphate)²¹. Since the high operating temperature increases the rate of reaction, it is expected to decrease the amount of phosphophyllite phase with increasing in bath temperature. It was reported that, increase in temperature leads to an increase in extent of metal dissolution¹⁶ which cause large crystals formation due to the more crystal growth. In addition, the high operating temperatures lead to the great conversion of soluble zinc phosphate to insoluble tertiary zinc phosphate and free phosphoric acid before the metal is treated¹⁴. The great regenerated phosphoric acid can damage the coating and cause crystal refinement. Under such condition, the coarse crystal and heavy deposit of coating produces that shows the inferior corrosion properties²⁸. Popić et al.²⁹ have investigated the effect of deposition temperature on the surface coverage and morphology of iron-phosphate coatings on low carbon steel. It has been shown that the increase in temperature of the phosphating bath up to 70 °C caused an increase in surface coverage. But in the presence of additive, the best surface coverage's was obtained at temperatures lower than 50 °C.

Electrochemical impedance was employed to confirm the anticorrosion behavior of the phosphate coating. Figure 2 shows the Nyquist plots of zinc phosphated steel obtained by 20 min immersion in phosphate solution in different operating temperatures. Impedance was measured at open circuit potential in 3.5%wt. NaCl solution. The data reveal that the impedance diagrams consist of a depressed capacitive loop which is due to the charge transfer resistance and double layer capacitance. The equivalent circuit compatible with the Nyquist diagram is depicted in Figure 3. In this electrical equivalent circuit, constant phase element Q_{DL} , R_s and R_{CT} can be corresponded to double layer capacitance, solution resistance and charge transfer resistance, respectively. To obtain a satisfactory impedance simulation of phosphate coated steel, it is necessary to replace the capacitor (C) with a constant phase element (CPE) Q in the equivalent circuit. The most widely accepted explanation for the presence of CPE behavior and depressed semicircles on solid electrodes is microscopic roughness, causing an inhomogeneous distribution in the solution resistance as well as in the double-layer capacitance^{30,31}.

To corroborate the equivalent circuit, the experimental data were fitted to equivalent circuit and the circuit elements were obtained. Table 2 illustrates the equivalent circuit parameters for the impedance spectra of phosphate coated steel in NaCl solution. The charge transfer resistances of the zinc phosphated samples significantly increase. From Table 2,

higher corrosion resistance is obtained with 45 °C coating temperature. This is due to the presence of the more uniform phosphate coating on the surface which decreases the active area of the substrate.

The low value of C_{DL} indicates the decrease in exposed area of electrode due to phosphate coatings. The Q_{DL} exponent (n) is a measure of the surface heterogeneity, and the low value indicates that the constant phase element is different

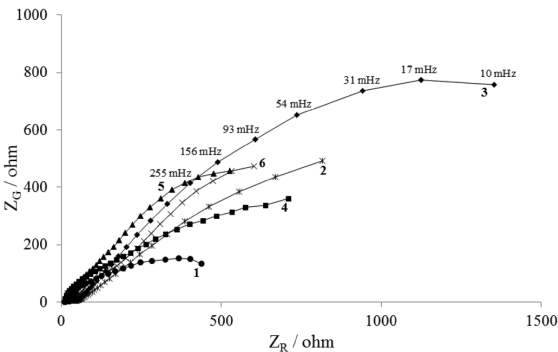


Figure 2. The Nyquist plots of steel electrode with and without zinc phosphate conversion coatings. Conversion coatings were obtained by 20 min immersion time in phosphate solution in different temperatures: 1) uncoated, 2) 20 °C, 3) 45 °C, 4) 55 °C, 5) 65 °C, 6) 80 °C.

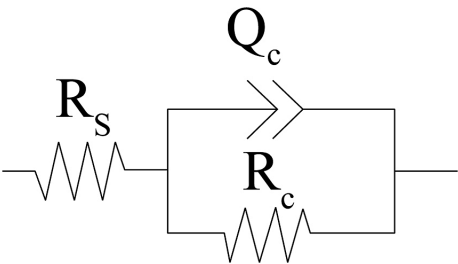


Figure 3. Equivalent circuits compatible with the experimental impedance data in Figure 2 for corrosion of zinc phosphate coated steel electrode.

Table 2. Impedance parameters of different operating temperature for the phosphate coatings in 3.5 wt. % NaCl solution. Coatings were prepared by 20 min immersion time in phosphate solution. The error obtained through fitting is presented for each element as (%).

Phosphate coating	$R_s (\pm 10) / \text{ohm}$	$Q_{DL} (\pm 10^{-3}) / \Omega^{-1} \text{cm}^{-2} \text{s}^n$	$C_{DL} (\pm 10^{-3}) / \text{F}$	$n (\pm 10^{-2})$
uncoated	605 (2%)	0.015 (3%)	0.061	0.61 (2%)
20 °C, 20 min	1842(4%)	0.015 (2%)	0.105	0.63 (1%)
45 °C, 20 min	2566(5%)	0.012 (5%)	0.056	0.69 (6%)
55 °C, 20 min	1421(1%)	0.015 (1%)	0.137	0.58 (6%)
65 °C, 20 min	1632(2%)	0.019 (1%)	0.096	0.68 (2%)
80 °C, 20 min	1687(2%)	0.018 (1%)	0.083	0.69 (5%)

from perfect capacitance. The values of n in Table 1 indicate that the electrode surface becomes more homogeneous with 45 °C coating temperature.

3.2. Effect of immersion time on corrosion performance

The polarization curves of phosphate coatings obtained in different immersion time in the phosphating bath at 45 °C are given in Figure 4. The corresponding corrosion parameters in 3.5% NaCl solution are presented in Table 3. It can be seen that by increasing immersion time from 5 to 20 min, I_{corr} and corrosion rate of the coated samples decrease. But in higher immersion times, 30 min, corrosion current density and corrosion rate increases. In low immersion time, the conversion coating formation is in the induction stage⁷ and the surface is attacked by H^+ ions presented in phosphating bath. This lead to increasing the corrosion rate. Therefore, at this immersion time, weak coating forms and in addition, the carbon steel surface is attacked by ions. With increasing the immersion time, the phosphate layer has enough time to settle on the steel surface, and produce a proper thickness for corrosion protection. In this immersion time, phosphate coats steel surface completely. But if the immersion time is too long, the quality and protective properties of coating decreases due to growth of phosphate crystals in the coating. This lead to the internal stress which decreases its toughness and increases porosity and cracking.

Fouladi & Amadeh³² have investigated the effect of phosphating time on microstructure and corrosion behavior of magnesium phosphate coating. The results indicated that increasing the phosphating time, enhanced both thickness and uniformity of the coating. The best results were observed after 20 min of phosphating.

Nyquist plots for the phosphate conversion coating obtained by 45 °C operating temperature in different immersion times are presented in Figure 5. Impedance data were measured at open circuit potential in 3.5%wt NaCl solution. All coatings show capacitive loop attributed to the double layer capacitance and the charge transfer resistance. To obtain a satisfactory simulation, the capacitor was replaced with a constant phase element. The experimental data were fitted to the equivalent circuit (Figure 3) and the circuit elements were obtained. Table 4 illustrates the equivalent circuit parameters for the impedance spectra of the phosphate coated steel obtained in different immersion times. According to Table 4, the charge transfer resistance increases in the presence of phosphate coatings. In addition, with increasing immersion times, the corrosion resistance increases due to the completion of

phosphate layer. As can be seen, higher corrosion resistance is obtained in 20 min immersion time. This is in agreement with the potentiodynamic polarization data.

3.3. Morphology and composition of the coating

The SEM images of phosphate conversion coatings obtained by 20 min immersion time in phosphate solution in different temperatures are presented in Figure 6. According

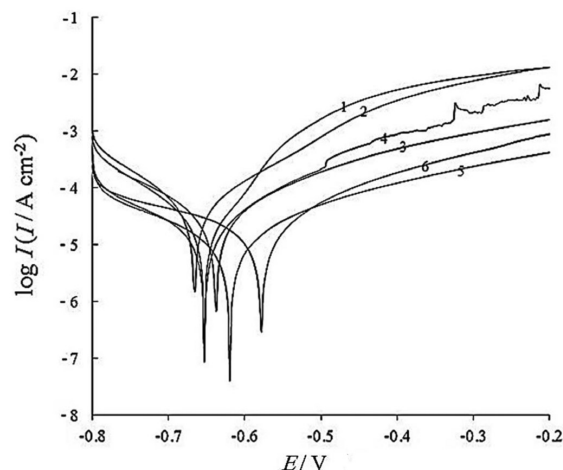


Figure 4. Polarization curves of steel electrode with and without zinc phosphate conversion coatings. Conversion coatings were obtained at 45 °C in phosphate solution with different immersion times: 1) uncoated, 2) 5 min, 3) 10 min, 4) 15 min, 5) 20 min, 6) 30 min.

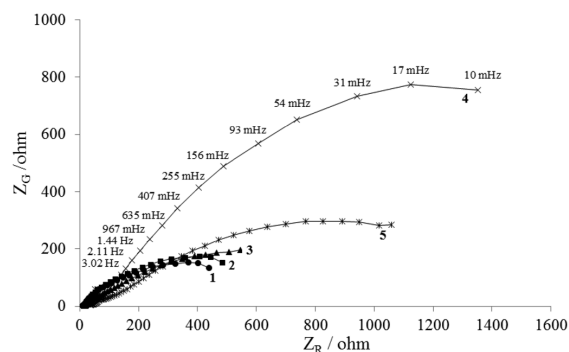


Figure 5. The Nyquist plots of steel electrode with and without zinc phosphate conversion coatings. Conversion coatings were obtained at 45 °C in phosphate solution with different immersion times: 1) uncoated, 2) 5 min, 3) 10 min, 4) 15 min, 5) 20 min, 6) 30 min.

Table 3. Potentiodynamic polarization parameters of different immersion times for the phosphate coatings in 3.5 wt. % NaCl solution. Coatings were prepared by immersion in phosphate solution in 45 °C.

Phosphate coating	$B_a (\pm 10^{-3})$ / V dec ⁻¹	$B_c (\pm 10^{-3})$ / V dec ⁻¹	$I_{corr} (\pm 5 \times 10^{-7})$ / A cm ⁻²	$E_{corr} (\pm 10^{-3})$ / V	$R_p (\pm 5)$ / ohm	Corr.rate ($\pm 10^{-3}$) / mpy
uncoated	0.114	0.094	2.89×10^{-5}	-0.653	772.995	3.39×10^{-1}
45 °C, 5 min	0.104	0.132	3.80×10^{-5}	-0.666	664.513	4.45×10^{-1}
45 °C, 10 min	0.140	0.188	3.01×10^{-5}	-0.638	1155.662	3.54×10^{-1}
45 °C, 15 min	0.160	0.138	1.58×10^{-5}	-0.653	2032.394	1.85×10^{-1}
45 °C, 20 min	0.137	0.110	6.49×10^{-6}	-0.620	4078.901	7.62×10^{-2}
45 °C, 30 min	0.189	0.108	1.11×10^{-5}	-0.578	2676.457	1.30×10^{-1}

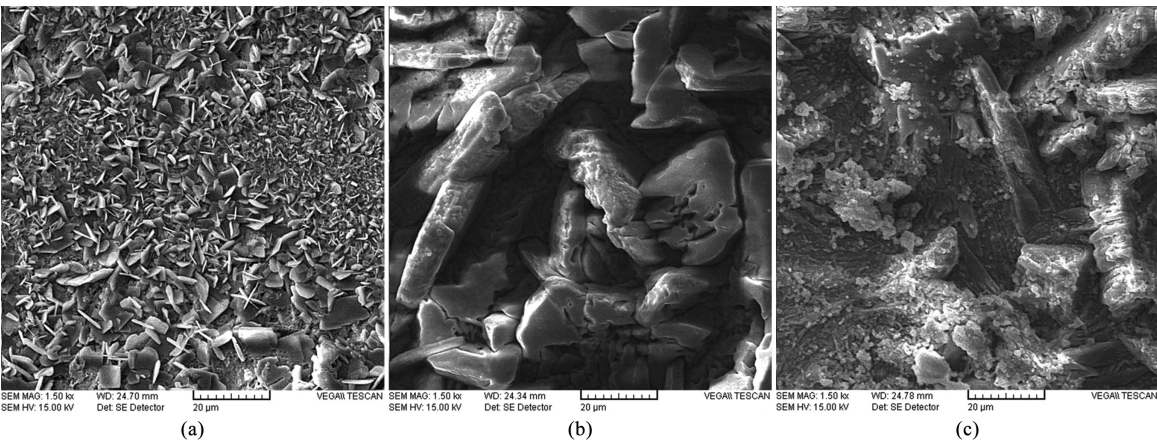


Figure 6. SEM images of zinc phosphate conversion coatings obtained by 20 min immersion in phosphate solution in different coating temperatures: (a) 45 °C, (b) 65 °C and (c) 80 °C.

Table 4. Impedance parameters of different immersion times for the phosphate coatings in 3.5 wt. % NaCl solution. Coatings were prepared by immersion in phosphate solution in 45 °C. The error obtained through fitting is presented for each element as (%).

Phosphate coating	$R_t (\pm 10)$ / ohm	$Q (\pm 10^{-3})$ / $\Omega^{-1}cm^{-2}s^n$	$C_{dl} (\pm 10^{-3})$ / F	$n (\pm 10^{-2})$
uncoated	605 (2%)	0.015 (3%)	0.061	0.61 (2%)
45 °C, 10 min	685 (5%)	0.014 (5%)	0.067	0.59 (1%)
45 °C, 15 min	1043 (5%)	0.008 (2%)	0.073	0.49 (2%)
45 °C, 20 min	2566(5%)	0.012 (5%)	0.056	0.69 (6%)
45 °C, 30 min	1464 (4%)	0.003 (3%)	0.012	0.51 (7%)

to observations, the phosphate coating obtained from 45 °C operating temperature, has finer and tiny crystals which result in continuous and compact structure. The coarse crystal and heavy deposit of coating is produced in higher operating temperatures that shows the inferior corrosion properties²⁸. At high operating temperature the great regenerated phosphoric acid could damage the coating and cause crystal refinement¹⁴.

The SEM images of phosphate conversion coatings obtained by 45 °C operating temperature in different immersion times in phosphate solution are represented in Figure 7. As can be seen, in low immersion time, the formation of phosphate coating is in the induction stage²³ and incomplete phosphate coating forms. Besides, the surface is attacked by phosphoric acid and causes the inferior corrosion behavior (Figure 7a). As shown in Figure 6a, with increasing immersion time, the phosphate crystals grow and uniform and compact coatings are obtained.

In the very high immersion time (Figure 7b), the more growth are observed in phosphate crystals and some cracks create in SEM image. This can be an evidence of high growth of crystals in coating and lead to decreasing the corrosion resistance. With increasing immersion times, the crystals may be cracked due to the presence of stresses between crystal layers during drying process. By withdrawing samples

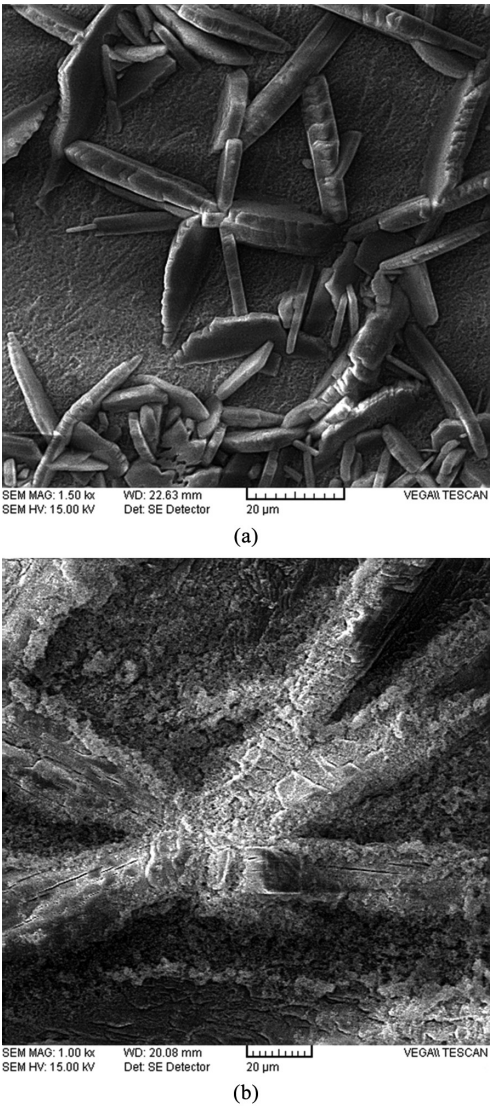


Figure 7. SEM images of zinc phosphate conversion coatings obtained at 45 °C in phosphate solution with different immersion times: (a) 5 min and (b) 30 min.

from the solution and drying them at ambient temperature, cracks progress on their surface and decrease the corrosion resistance of the coatings. In addition, the high immersion time give this ability to regenerated phosphoric acid to refine and damage the phosphate crystals. The EDX analysis of zinc phosphate coated steel electrode obtained by 20 min immersion in phosphate solution at 45 °C is presented in Figure 8 and the corresponding elemental analysis are obtained as O: 18.4, P: 6.1, Fe: 60.2 and Zn: 15.3%wt.

Figure 9 shows SEM images of the surface of the zinc phosphate conversion coatings of steel electrodes after polarization test. Zinc phosphate coatings were obtained by 45 °C operating temperature in different immersion times in coatings solution. As seen, more uniform coating surface is observed for coating obtained by 20 min immersion time which is due to the lower current in anodic branch of polarization. High immersion time lead to creating the internal stress which increases the pores and cracks and decreases corrosion resistance in corrosive solution.

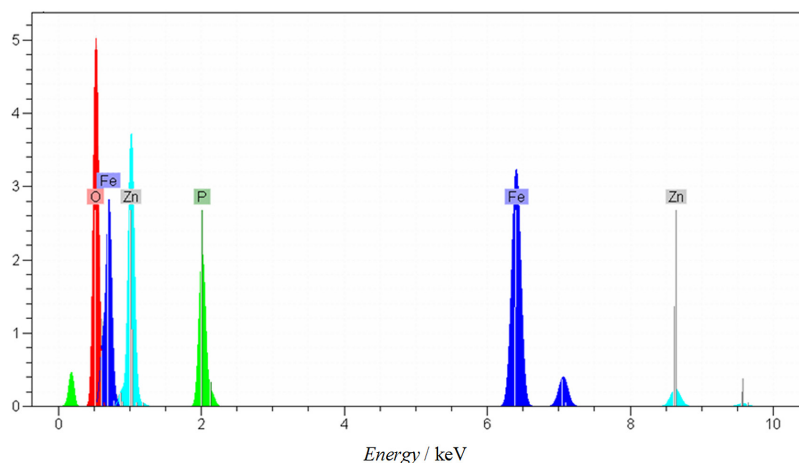


Figure 8. EDS spectra of the phosphate conversion layer obtained by 20 min immersion in phosphate solution at 45 °C.

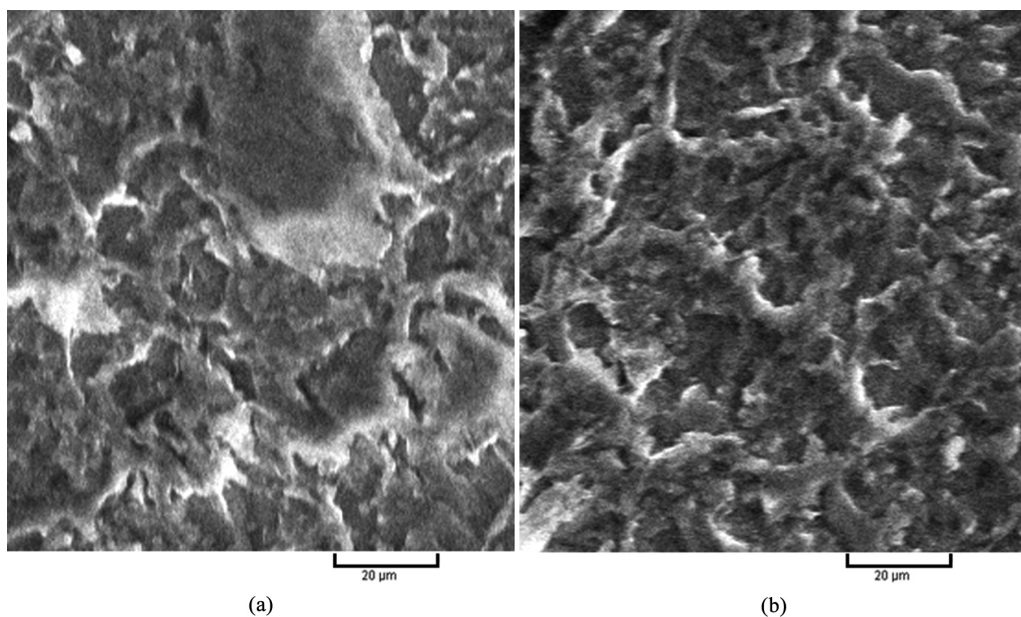


Figure 9. SEM images of zinc phosphate conversion coatings after polarization test obtained at 45 °C in phosphate solution with different immersion times: (a) 20 min and (b) 30 min.

4. Conclusion

The corrosion behavior of phosphate conversion coatings applied on steel surface was investigated in 3.5 wt. % NaCl solution. This conversion coating improved the corrosion

resistance of the steel due to the formation of barrier film. The potentiodynamic polarization studies showed that the anodic and cathodic currents were decreased and the polarization resistance increased in the presence of zinc phosphating. The phosphating temperature played an important role to

provide phosphate conversion coating and the best corrosion resistance was obtained with 45 °C operating temperature. In addition, the corrosion resistance was increased with increasing the immersion time due to the increasing of the

phosphate coating continuity and compactness. The results of SEM showed that the phosphate coatings, obtained from 20 min immersion time ratio in 45 °C operating temperature, were more uniform and continuous.

References

- Gunes I, Erdogan M and Çelik AG. Corrosion behavior and characterization of plasma nitrided and borided AISI M2 steel. *Materials Research*. 2014; 17(3):612-618. <http://dx.doi.org/10.1590/S1516-14392014005000061>.
- Forero AB, Núñez MMG and Bott IS. Analysis of the corrosion scales formed on API 5L X70 and X80 steel pipe in the presence of CO₂. *Materials Research*. 2014; 17(2):461-471. <http://dx.doi.org/10.1590/S1516-14392013005000182>.
- Silva WDM, Carneiro JRG and Trava-Airoldi VJ. XPS, XRD and laser raman analysis of surface modified of 6150 steel substrates for the deposition of thick and adherent diamond-like carbon coatings. *Materials Research*. 2013; 16(3):603-608. <http://dx.doi.org/10.1590/S1516-14392013005000027>.
- Jafari H, Danaee I, Eskandari H and RashvandAvei M. Electrochemical and quantum chemical studies of N,N-bis(4-hydroxybenzaldehyde)-2,2-dimethylpropanediimine Schiff base as corrosion inhibitor for low carbon steel in HCl solution. *Journal of Environmental Science and Health. Part A*. 2013; 48:1628-1641. <http://dx.doi.org/10.1080/10934529.2013.815094>. PMID: 23947700.
- Tomachuk CR, Elsner CI and Di Sarli AR. Electrochemical characterization of chromate free conversion coatings on electrogalvanized steel. *Materials Research*. 2014; 17(1):61-68. <http://dx.doi.org/10.1590/S1516-14392013005000179>.
- Acchar W, Barreto LS, Paes HR Jr, Cruz CR and Feistauer EE. LaCrO₃ composite coatings for AISI 444 stainless steel solid oxide fuel cell interconnects. *Materials Research*. 2012; 15(6):1064-1069. <http://dx.doi.org/10.1590/S1516-14392012005000140>.
- Saliba-Silva AM, Oliveira MCLD and Costa I. Effect of molybdate on phosphating of Nd-Fe-B magnets for corrosion protection. *Materials Research*. 2005; 8(2):147-150. <http://dx.doi.org/10.1590/S1516-14392005000200009>.
- Bahri H, Danaee I and Rashed GR. The effect of curing time and curing temperature on the corrosion behavior of nanosilica modified potassium silicate coatings on AA2024. *Surface and Coatings Technology*. 2014; 254:305-312. <http://dx.doi.org/10.1016/j.surfcoat.2014.06.041>.
- Danaee I, Zamanizadeh HR, Fallahi M and Lotfi B. The effect of surface pre-treatments on corrosion behavior of cerium-based conversion coatings on Al 7075-T6. *Materials and Corrosion*. 2014; 65(8):815-819. <http://dx.doi.org/10.1002/maco.201307147>.
- Souza MEP, Ariza E, Ballester M, Yoshida IVP, Rocha LA and Freire CMA. Characterization of organic-inorganic hybrid coatings for corrosion protection of galvanized steel and electroplated ZnFe steel. *Materials Research*. 2006; 9(1):59-64. <http://dx.doi.org/10.1590/S1516-14392006000100012>.
- Cunha CA, Lima NB, Martinelli JR, Bressiani AHA, Padial AGF and Ramanathan LV. Microstructure and mechanical properties of thermal sprayed nanostructured Cr₃C₂-Ni₂₀Cr coatings. *Materials Research*. 2008; 11(2):137-143. <http://dx.doi.org/10.1590/S1516-14392008000200005>.
- Brandolt CS, Souza JG Jr, Kunst SR, Vega MRO, Schroeder RM and Malfatti CF. Niobium and niobium-iron coatings on API 5LX 70 steel applied with HVOF. *Materials Research*. 2014; 17(4):866-877. <http://dx.doi.org/10.1590/S1516-14392014005000087>.
- Lazar AM, Yespica WP, Marcelin S, Pébère N, Samélor D, Tendero C, et al. Corrosion protection of 304L stainless steel by chemical vapor deposited alumina coatings. *Corrosion Science*. 2014; 81:125-131. <http://dx.doi.org/10.1016/j.corsci.2013.12.012>.
- Jegannathan S, Sankara Narayanan TSN, Ravichandran K and Rajeswari S. Evaluation of the corrosion resistance of phosphate coatings obtained by anodic electrochemical treatment. *Progress in Organic Coatings*. 2006; 57(4):392-399. <http://dx.doi.org/10.1016/j.porgcoat.2006.09.023>.
- Sankara Narayanan TSN, Jegannathan S and Ravichandran K. Corrosion resistance of phosphate coatings obtained by cathodic electrochemical treatment: Role of anode-graphite versus steel. *Progress in Organic Coatings*. 2006; 55(4):355-362. <http://dx.doi.org/10.1016/j.porgcoat.2006.01.009>.
- Jegannathan S, Sankara Narayanan TSN, Ravichandran K and Rajeswari S. Formation of zinc phosphate coating by anodic electrochemical treatment. *Surface and Coatings Technology*. 2006; 200(20-21):6014-6021. <http://dx.doi.org/10.1016/j.surfcoat.2005.09.017>.
- Arthanareeswari M, Sankara Narayanan TSN, Kamaraj P and Tamilselvi M. Influence of galvanic coupling on the formation of zinc phosphate coating. *Indian Journal of Chemical Technology*. 2010; 17:167-175.
- Jegannathan S, Sankara Narayanan TSN, Ravichandran K and Rajeswari S. Performance of zinc phosphate coatings obtained by cathodic electrochemical treatment in accelerated corrosion tests. *Electrochimica Acta*. 2005; 51(2):247-256. <http://dx.doi.org/10.1016/j.electacta.2005.04.020>.
- Kouisni L, Azzi M, Dalard F and Maximovitch S. Phosphate coatings on magnesium alloy AM60 Part 2: Electrochemical behaviour in borate buffer solution. *Surface and Coatings Technology*. 2005; 192:239-246.
- Sheng M, Wang Y, Zhong Q, Wu H, Zhou Q and Lin H. The effects of nano-SiO₂ additive on the zinc phosphating of carbon steel. *Surface and Coatings Technology*. 2011; 205(11):3455-3460. <http://dx.doi.org/10.1016/j.surfcoat.2010.12.011>.
- Ashassi-Sorkhabi H, Seifzadeh D and Harrafi H. Phosphatation of Iron Powder Metallurgical Samples for Corrosion Protection. *Journal of the Indian Chemical Society*. 2007; 4:72-77.
- Bikulčius G, Burokas V, Martušienė A and Matulionis E. Effects of magnetic fields on the phosphating process. *Surface and Coatings Technology*. 2003; 172:139-143. [http://dx.doi.org/10.1016/S0257-8972\(03\)00388-8](http://dx.doi.org/10.1016/S0257-8972(03)00388-8).
- Sankara Narayanan TSN. Surface pretreatment by phosphate conversion coatings – a review. *Reviews on Advanced Materials Science* 2005; 9(5):130-177.
- Jegannathan S, Sankara Narayanan TSN, Ravichandran K and Rajeswari S. Formation of zinc-zinc phosphate composite coatings by cathodic electrochemical treatment. *Surface and Coatings Technology*. 2006; 200(12-13):4117-4126. <http://dx.doi.org/10.1016/j.surfcoat.2005.04.022>.
- Danaee I. Kinetics and mechanism of palladium electrodeposition on graphite electrode by impedance and noise measurements.

- Journal of Electroanalytical Chemistry*. 2011; 662(2):415-420. <http://dx.doi.org/10.1016/j.jelechem.2011.09.012>.
26. Macdonald JR. Note on the parameterization of the constant phase admittance element. *Solid State Ionics*. 1984; 13(2):147-149. [http://dx.doi.org/10.1016/0167-2738\(84\)90049-3](http://dx.doi.org/10.1016/0167-2738(84)90049-3).
27. Gholami M, Danaee I, Maddahy MH and RashvandAvei M. Correlated ab Initio and electroanalytical study on inhibition behavior of 2Mercaptobenzothiazole and its thiole–thione tautomerism effect for the corrosion of steel (API 5L X52) in Sulphuric Acid Solution. *Industrial & Engineering Chemistry Research*. 2013; 52(42):14875-14889. <http://dx.doi.org/10.1021/ie402108g>.
28. Sankara Narayanan TSN and Subbaiyan M. Overheating—its decisive role in phosphating. *Metal Finishing*. 1995; 93(1):30-31. [http://dx.doi.org/10.1016/0026-0576\(95\)91149-h](http://dx.doi.org/10.1016/0026-0576(95)91149-h).
29. Popić JP, Jegdić BV, Bajat JB, Veljović Đ, Stevanović SI and Mišković-Stanković VB. The effect of deposition temperature on the surface coverage and morphology of iron-phosphate coatings on low carbon steel. *Applied Surface Science*. 2011; 257:10855-10862.
30. Jafari H, Danaee I, Eskandari H and RashvandAvei M. Electrochemical and theoretical studies of adsorption and corrosion Inhibition of N,N'-Bis(2-hydroxyethoxyacetophenone)-2,2-dimethyl-1,2-propanediimine on low carbon steel (API 5L Grade B) in acidic solution. *Industrial & Engineering Chemistry Research*. 2013; 52(20):6617-6632. <http://dx.doi.org/10.1021/ie400066x>.
31. Danaee I, Niknejad Khomami M and Attar AA. Corrosion behavior of AISI 4130 steel alloy in ethylene glycolewater mixture in presence of molybdate. *Materials Chemistry and Physics*. 2012; 135(2-3):658-667. <http://dx.doi.org/10.1016/j.matchemphys.2012.05.041>.
32. Fouladi M and Amadeh A. Effect of phosphating time and temperature on microstructure and corrosion behavior of magnesium phosphate coating. *Electrochimica Acta*. 2013; 106:1-12. <http://dx.doi.org/10.1016/j.electacta.2013.05.041>.